

Optical, electrochemical and structural studies of the first rhenium compound of di-2-pyridylketone benzoylhydrazone (dpkbz) *fac*- $\text{Re}(\text{CO})_3(\text{dpkbh})\text{Cl}$

Mohammed Bakir*, Ordel Brown

Department of Chemistry, The University of the West Indies, Mona Campus, Kingston 7, Jamaica

Received 21 October 2002; accepted 2 April 2003

Abstract

The reaction between $\text{Re}(\text{CO})_5\text{Cl}$ and di-2-pyridylketone benzoylhydrazone (dpkbh) in refluxing toluene gave *fac*- $\text{Re}(\text{CO})_3(\text{dpkbh})\text{Cl}$ in good yield. Spectroscopic and electrochemical measurements on *fac*- $\text{Re}(\text{CO})_3(\text{dpkbh})\text{Cl}$ revealed strong solvent–solute interaction, as manifested by the sensitivity of its reduction potentials and electronic absorption spectra to solvent variations. Spectroscopic and thermo-optical measurements in polar solvents in the presence of NaBH_4 and NaBF_4 , or NaOH and citric acid reveal reversible interconversion between the low- and high-energy electronic states of *fac*- $\text{Re}(\text{CO})_3(\text{dpkbh})\text{Cl}$ at 440 and 318 nm. Electrochemical measurements on *fac*- $\text{Re}(\text{CO})_3(\text{dpkbh})\text{Cl}$ show irreversible redox processes pointing to electrochemical transformations following the first electronic transfer(s). Crystals of *fac*- $\text{Re}(\text{CO})_3(\text{dpkbh})\text{Cl}$ obtained from an acetonitrile solution of *fac*- $\text{Re}(\text{CO})_3(\text{dpkbh})\text{Cl}$ are centric and crystals of *fac*- $\text{Re}(\text{CO})_3(\text{dpkbh})\text{Cl}\cdot\text{dmsO}$ obtained from a dmsO solutions of *fac*- $\text{Re}(\text{CO})_3(\text{dpkbh})\text{Cl}$ are acentric. Structural studies show non-identical twins of *fac*- $\text{Re}(\text{CO})_3(\text{dpkbh})\text{Cl}$ and *fac*- $\text{Re}(\text{CO})_3(\text{dpkbh})\text{Cl}\cdot\text{dmsO}$ with distorted octahedral coordination about rhenium and the conformation about the amide group is syn- in *fac*- $\text{Re}(\text{CO})_3(\text{dpkbh})\text{Cl}$ and anti- in *fac*- $\text{Re}(\text{CO})_3(\text{dpkbh})\text{Cl}\cdot\text{dmsO}$. The packing of molecules shows a web of hydrogen bonds that may account for the stability of different conformations observed in the solid state.

© 2003 Elsevier B.V. All rights reserved.

Keywords: Rhenium; Di-2-pyridyl ketone; Hydrazone; Optosensing

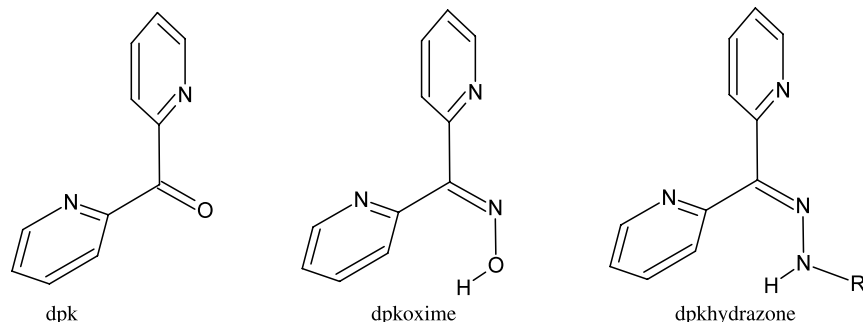
1. Introduction

Di-2-pyridyl ketone (dpk), its oxime (dpkoxime), and hydrazone (dpkhydrazone) derivatives are of interest for their physico-chemical properties, reactivity patterns and applications in many processes that include molecular recognition and catalysis [1–10]. Several coordination modes were reported for dpk and its derivatives that include monodentate binding through an N atom of one pyridyl ring, as in $[\text{Ag}(\text{dpkoxime})]\text{NO}_2$, bidentate binding through the N atoms of the pyridyl rings as in *fac*- $\text{Re}(\text{CO})_3(\text{dpk})\text{Cl}$ or through an N atom of one pyridine ring and the N atom of the backbone as in $[\text{Co}(\text{dpkO},\text{OH})(\text{dpkoxime})]\text{NO}_2\cdot\text{H}_2\text{O}$ where dpkO,OH

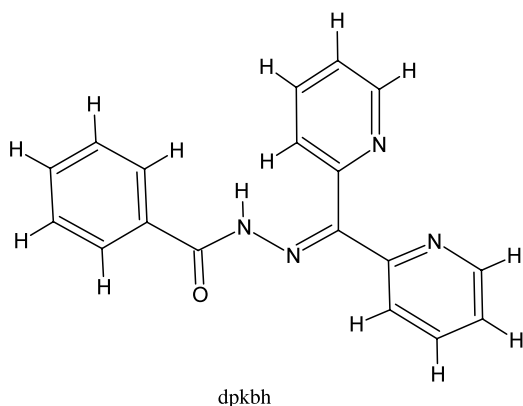
is hydroxydi(2-pyridyl)methoxide and tridentate through the nitrogen atoms of the pyridine rings and the oxygen atom of the methoxide moiety of dpkO,OH as in *fac*- $\text{Re}(\text{CO})_3(\text{dpkO},\text{OH})$ [6–8,11].

We have been interested in the chemistry of di-2-pyridyl-like ligands and have described the synthesis, optical, electrochemical and structures of a variety of dpk derivatives and their metal compounds [11–24]. Optical and thermodynamic measurements on dpk hydrazones that include di-2-pyridylketone benzoylhydrazone (dpkbh) in polar non-aqueous solvents revealed reversible interconversion between two interlocked electronic states due to different conformational forms of the hydrazone backbone resulted from intermolecular interaction between these species and their surroundings [15,20,21]. The high values for the extinction coefficients and low values for the activation parameters for the interconversion between the low- and high-energy

* Corresponding author. Tel.: +876-935-8164; fax: +876-977-1835.
E-mail address: mohammed.bakir@uwimona.edu.jm (M. Bakir).



electronic states of dpk hydrazones in polar non-aqueous solvents allowed for the use of these systems (dpk hydrazones and surrounding molecules) as molecular sensors for a variety of chemical stimuli that include metal ions and biomolecules [15,20,21]. X-ray structural analysis on a series of dpk hydrazones revealed the presence of a web of non-covalent interactions that include solvent–solute, solute–solute, and π -stacking, which may account for their interlocked charge-transfer bands and molecular sensitivity [17,19,21–24]. Although, dpkbh is widely used as a sensitive analytical reagent for the optical determination of trace amounts of metal ions, and in a recent report, we described its optosensing behavior in non-aqueous media, to our knowledge there has been no report on the isolation of any of its metal compounds [21].



In this report, we describe the synthesis of the first metal carbonyl compound of dpkbh along with its optical, electrochemical and structural properties. Studies of this nature are important as a variety of hydrazones are used in non-linear optics and molecular recognition and solvent variations and the presence of organized non-covalent hydrogen bonds in materials was recognized by many authors to lead to the formation of polar chains and their appropriate packing may lead to the generation of acentric crystals required for non-linear optical responses, e.g. second harmonic generation [25–28].

2. Experimental

2.1. Reagents and reaction procedures

Solvents were reagent grade and thoroughly deoxygenated prior to use. All other reagents were obtained from commercial sources and used without further purification. The ligand dpkbh, melting point 141–142 °C was prepared by refluxing a mixture of dpk, benzhydrazide, EtOH, and two drops of HCl using a standard procedure as described previously for the synthesis of several dpk hydrazones that include dpkbh [21]. All reactions were performed under a nitrogen atmosphere.

2.2. Preparation of *fac*-Re(dpkbh)(CO)₃Cl

A mixture of Re(CO)₅Cl (200 mg, 0.55 mmol), dpkbh (220 mg, 0.73 mmol) and toluene (50 ml) was refluxed for 10 h. The resulting reaction mixture was allowed to cool to room temperature and reduced in volume to ~ 25 ml. An off-yellow solid was filtered off, washed with hexane, diethyl ether, and dried; yield 240 mg (72%) (Found: C, 41.18; H, 2.37; Cl, 8.99. C₂₁H₁₄Cl N₄O₄Re requires C, 41.48; H, 2.32; Cl, 9.22%). Infrared data (KBr disk, cm⁻¹): $\nu(\text{C}\equiv\text{O})$ 2016, 1907, 1870; $\nu(\text{C}=\text{O})$ 1655 and $\nu(\text{N}-\text{H})$ 3156, 3130, 3067, 3035 and $\nu(\text{C}-\text{H})$ 2883. ¹H NMR (δ ppm): in dmsO-d₆ 12.08 (s, 1H, NH), 9.02 (d, 1H, dpk), 8.90 (d, 1H, dpk), 8.24 (overlapped t's, 2H dpk), 8.11 (d, 1H, dpk), 7.97 (d, 1H, dpk), 7.74 (m, 4H, ph), 7.50 (m, 3H, 1H ph, and 2H dpk). UV–Vis {CH₂Cl₂, λ (nm), (ϵ , cm⁻¹ M⁻¹)}: 310 (24 840 ± 2000).

2.3. Physical measurements

Electronic absorption spectra were recorded on a Perkin–Elmer Lambda 19 UV–Vis–NIR spectrometer. Solution ¹H NMR spectra were recorded on a Bruker ACE 200-MHz Fourier-transform spectrometer and referenced to the residual protons in the incompletely

deuteriated solvent. Infrared spectra were recorded as KBr pellets on a Perkin–Elmer Spectrum 1000 FT-IR Spectrometer. Electrochemical measurements were performed with the use of a Princeton Applied Research (PAR) Model 173 potentiostat/galvanostat and Model 276 interface in conjunction with a 286 PC. Data were acquired with the EG&G PARC Headstart program and manipulated using the Microsoft Excel Program. Measurements were performed in solutions that were 0.1 M in $[N(n\text{-Bu})_4](PF_6)$. The $E_{p,a}$, $E_{p,c}$ and $E_p = (E_{p,a} + E_{p,c})/2$ values were referenced to the potassium chloride saturated calomel electrode (SCE), at room temperature and are uncorrected for junction potentials. The number of electrons on the redox waves was determined using the oxidative peak current of the reversible one-electron couple of $FeCp_2/FeCp_2^+$ couple as an internal standard. Electrochemical cells were of conventional design based on scintillation vials or H-cells. A glassy-carbon disc was used as the working electrode and Pt-wire as a counter electrode.

2.4. X-ray crystallography

Yellow crystals of $fac\text{-Re}(\text{CO})_3(\text{dpkbh})\text{Cl}$ and $fac\text{-Re}(\text{CO})_3(\text{dpkbh})\text{Cl}\cdot\text{dmsO}$ were obtained from acetonitrile and dmsO solutions of $fac\text{-Re}(\text{CO})_3(\text{dpkbh})\text{Cl}$ when allowed to stand at room temperature for several days. Single crystals were selected and mounted on glass fibers with epoxy cement. A Bruker AXS with a Mo $K\alpha$ radiation and a graphite monochromator was used for data collection and the SHELXTL software package version 5.1 was used for structure solution [29,30]. Cell parameters and other crystallographic information are given in Table 1 along with additional details concerning data collection.

2.5. Analytical procedures

Elemental microanalyses were performed by MEDAC Ltd, Department of Chemistry, Brunel University, Uxbridge, United Kingdom.

3. Results and discussion

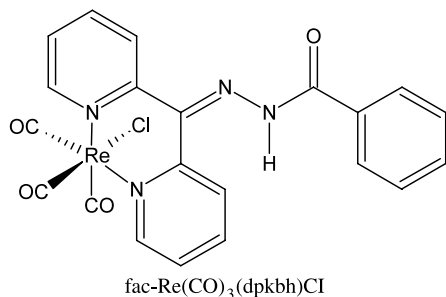
When $\text{Re}(\text{CO})_5\text{Cl}$ was allowed to react with dpkbh in refluxing toluene, $fac\text{-Re}(\text{CO})_3(\text{dpkbh})\text{Cl}$ was isolated in good yield. This reaction is similar to those reported for the synthesis of rhenium tricarbonyl compounds of the type $fac\text{-Re}(\text{CO})_3(\text{L-L})\text{Cl}$ where L-L = bidentate α -diimine ligand from the reaction between $\text{Re}(\text{CO})_5\text{Cl}$ and L-L in refluxing toluene [11,14]. The formulation of the isolated rhenium-carbonyl compound as $fac\text{-Re}(\text{CO})_3(\text{dpkbh})\text{Cl}$ is based on the results of a number of spectroscopic measurements and a comparison of these results with those reported for $fac\text{-}$

Table 1
Crystal data and structure refinement for $fac\text{-Re}(\text{CO})_3(\text{dpkbh})\text{Cl}$ and $fac\text{-Re}(\text{CO})_3(\text{dpkbh})\text{Cl}\cdot\text{dmsO}$

Compound	<i>fac</i> - $\text{Re}(\text{CO})_3(\text{dpkbz})\text{Cl}$	<i>fac</i> - $\text{Re}(\text{CO})_3(\text{dpkbz})\text{Cl}\cdot$ dmsO
Empirical formula	$\text{C}_{21}\text{H}_{14}\text{ClN}_4\text{O}_4\text{Re}$	$\text{C}_{23}\text{H}_{20}\text{ClN}_4\text{O}_5\text{SRe}$
Formula weight	608.01	686.14
Crystal system	triclinic	triclinic
Space group	$P\bar{1}$	$P\bar{1}$
<i>Unit cell dimensions</i>		
<i>a</i> (Å)	12.17(9)	9.04(12)
<i>b</i> (Å)	13.42(17)	12.14(14)
<i>c</i> (Å)	13.75(10)	12.25(10)
α (°)	106.37(9)	80.17(8)
β (°)	90.00(4)	75.56(9)
γ (°)	90.00(9)	86.53(11)
<i>V</i> (Å ³)	2154.8(4)	1282.3(2)
<i>Z</i>	4	2
<i>D</i> _{calc} (mg m ⁻³)	1.874	1.777
Absorption coefficient (mm ⁻¹)	5.799	4.964
<i>F</i> (0 0 0)	1168	668
θ Range for data collection (°)	2.28–19.99	2.23–22.50
Reflections collected/unique	2788/2682	4098/4098
	[<i>R</i> _{int} = 0.0119]	[<i>R</i> _{int} = 0.0000]
Completeness to θ	19.99 (66.6%)	22.50 (99.7%)
Absorption correction	empirical	none
Max/min transmission	0.5603 and 0.2303	
Data/restraints/parameters	2682/0/530	4098/4/421
Goodness-of-fit on <i>F</i> ²	1.036	1.355
Final <i>R</i> indices [<i>I</i> > 2 σ (<i>I</i>)]	<i>R</i> ₁ = 0.0356	<i>R</i> ₁ = 0.0543
	<i>wR</i> ₂ = 0.1086	<i>wR</i> ₂ = 0.1375
<i>R</i> indices (all data)	<i>R</i> ₁ = 0.0410	<i>R</i> ₁ = 0.0551
	<i>wR</i> ₂ = 0.1158	<i>wR</i> ₂ = 0.1413
Absolute structure parameter		0.127(18)
Extinction coefficient	0.0016(3)	0.0005(7)
Largest difference peak and hole (e Å ⁻³)	0.791 and -0.789	2.970 and -4.051

Temperature = 298(2) K, wavelength = 0.71073 Å, refinement method, full-matrix least-squares on *F*².

$\text{Re}(\text{CO})_3(\text{dpknph})\text{Cl}$ where dpknph is dpk *p*-nitrophenylhydrazine and other related compounds [19,22]. In the IR spectrum of $fac\text{-Re}(\text{CO})_3(\text{dpkbh})\text{Cl}$, three strong bands appeared in the $\nu(\text{C}\equiv\text{O})$ stretching region similar to those reported for the carbonyl groups in $fac\text{-Re}(\text{CO})_3(\text{dpknph})\text{Cl}$ and other tricarbonylhalorhenium(I) compounds containing α -diimine ligands of the type $fac\text{-Re}(\text{CO})_3(\text{L-L})\text{Cl}$, and they confirmed the assigned *fac*-geometry [11,14,19]. The $\nu(\text{C}=\text{N})$ of the hydrazone moiety and the combined $\nu(\text{C}=\text{C})$ and $\nu(\text{C}=\text{N})$ of the pyridine vibrations are normal and in the same region as in $fac\text{-Re}(\text{CO})_3(\text{dpknph})\text{Cl}$ [19].



A strong and sharp stretching mode appeared at 1654 cm^{-1} due to the ketonic group of *N,N*-coordinated dpkbh. This band appeared at higher energy ($\sim 30\text{ cm}^{-1}$) compared to the ketonic stretching mode of dpkbh and is consistent with the decrease in electron density of the ketonic group upon *N,N*-coordination of dpkbh, hints to enhanced π -back bonding as a result of electron/charge delocalization across the metallocyclic ring and backbone of the hydrazone moiety, and is similar to those observed for the *N,N*-coordination of dpk [11]. In the $\nu(\text{NH})$ and $\nu(\text{C-H})$ stretching region of $\text{fac-Re}(\text{CO})_3(\text{dpkbh})\text{Cl}$, a series of weak and broad bands appeared between 3200 and 2800 cm^{-1} and for the free ligand, a sharp band appeared at 3060 cm^{-1} and a broad band appeared at 2920 cm^{-1} . The broad character of these bands and their appearance at $\leq 3200\text{ cm}^{-1}$ point to possible participation of these groups in hydrogen bonding [31]. The ^1H NMR spectra of $\text{fac-Re}(\text{CO})_3(\text{dpkbh})\text{Cl}$ in $\text{dms}\text{-d}_6$ shows $\delta(\text{N-H})$ at 12.08

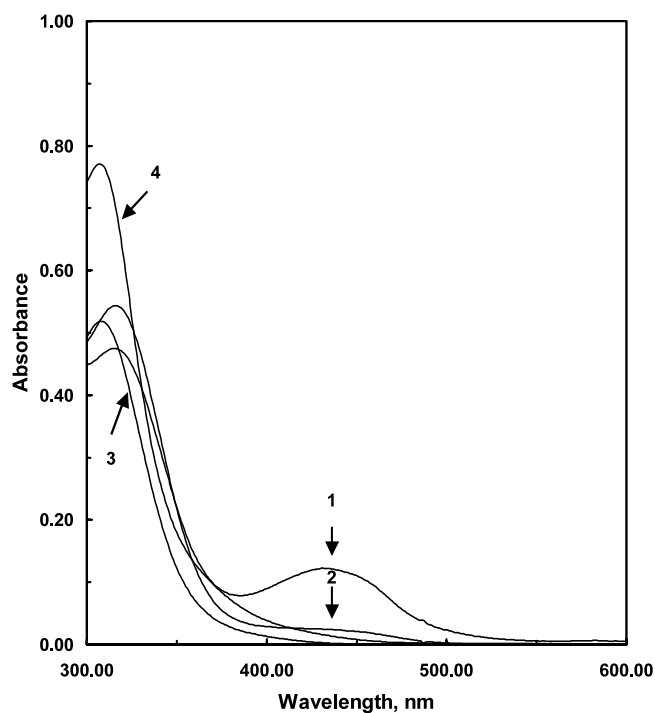


Fig. 1. Electronic absorption of $\text{fac-Re}(\text{CO})_3(\text{dpkbh})\text{Cl}$ in (1) dmso ($2.00 \times 10^{-5}\text{ M}$), (2) dmf ($2.00 \times 10^{-5}\text{ M}$), (3) CH_3CN ($2.60 \times 10^{-5}\text{ M}$) and (4) CH_2Cl_2 ($3.10 \times 10^{-5}\text{ M}$).

ppm and a series of resonances consistent with the coordinated dpkbh. No evidence of paramagnetic line broadening or unusual shifts of resonances appeared in the spectra of this compound confirming its diamagnetic character.

The electronic absorption spectra of $\text{fac-Re}(\text{CO})_3(\text{dpkbh})\text{Cl}$ in different solvents are shown in Fig. 1. These spectra show sensitivity of the absorption bands of $\text{fac-Re}(\text{CO})_3(\text{dpkbh})\text{Cl}$ to solvent variations as apparent from the change in position and intensity of the low energy ($\sim 440\text{ nm}$) and high-energy ($\sim 320\text{--}310\text{ nm}$) absorption bands in different solvents and point to solvent–solute interactions. In non-polar solvents such as CH_2Cl_2 , a single absorption band with extinction coefficient of $24840 \pm 2000\text{ M}^{-1}\text{ cm}^{-1}$ appeared at 310 nm , and in polar hydrogen bonding solvents such as dmf , two absorption bands appeared at 440 and 318 . A plot of the absorbance of the low and high-energy absorption bands at 440 and 318 nm versus total concentration in dmf is non-linear pointing to deviation from Beer's Law. As the concentration of $\text{fac-Re}(\text{CO})_3(\text{dpkbh})\text{Cl}$ decreases, the ratio of the low- and high-energy absorption bands increases, pointing to direct solvent–solute interaction and confirming the spectral results observed in Fig. 1. These spectral features are similar to those reported for dpkbh, $\text{fac-Re}(\text{CO})_3(\text{dpkphh})\text{Cl}$ where dpkphh is dpk phenylhydrazone and other related compounds although subtle difference are worth noting [21,22]. Compared to $\text{fac-Re}(\text{CO})_3(\text{dpkphh})\text{Cl}$

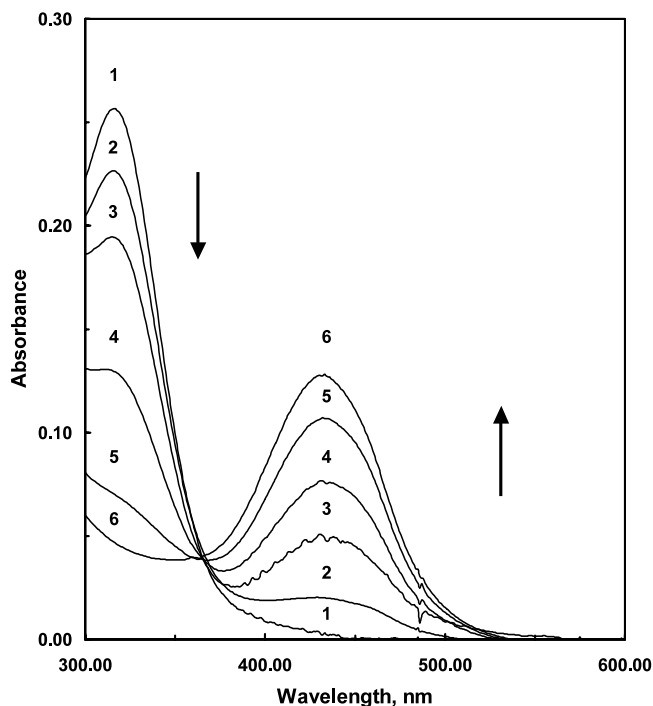


Fig. 2. Electronic absorption spectra of $1.00 \times 10^{-5}\text{ M}$ $\text{fac-Re}(\text{CO})_3(\text{dpkbh})\text{Cl}$ and $2.2 \times 10^{-1}\text{ M}$ NaBF_4 in dmso in the presence of $1.80 \times 10^{-4}\text{ M}$ (1), $2.2 \times 10^{-4}\text{ M}$ (2), $2.5 \times 10^{-5}\text{ M}$ (3), $5.0 \times 10^{-3}\text{ M}$ (4) and $1.20 \times 10^{-2}\text{ M}$ (5) NaBH_4 in dmso at 298 K .

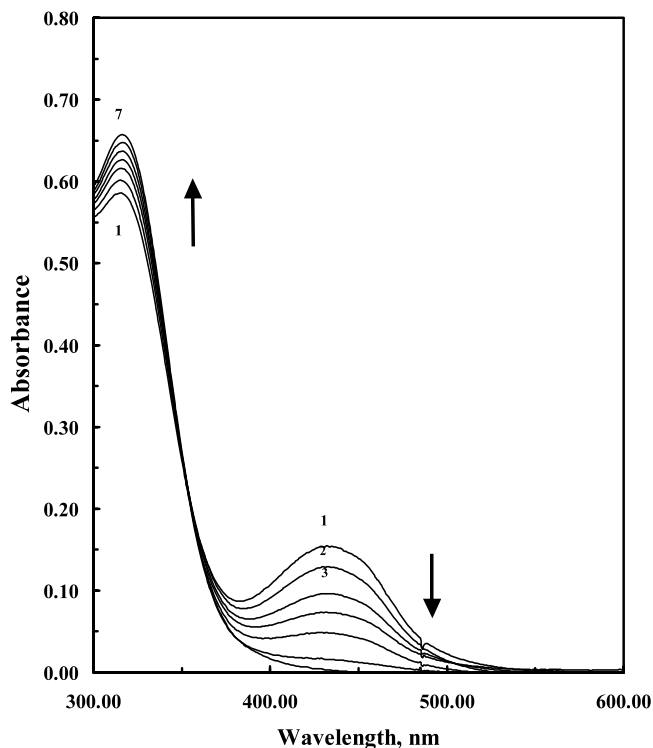
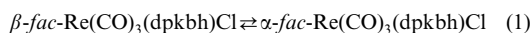


Fig. 3. Electronic absorption spectra of 3.00×10^{-5} M *fac*- $\text{Re}(\text{CO})_3(\text{dpkhh})\text{Cl}$ in dmsO (1) in the presence 1×10^{-9} M (2), 2×10^{-9} M (3), 5×10^{-9} M (4), 1×10^{-8} M (5), 2×10^{-8} M (6) and 5×10^{-8} M (7) in $\text{Mg}(\text{ClO}_4)_2$.

$\text{Re}(\text{CO})_3(\text{dpkhh})\text{Cl}$, the low energy absorption bands of *fac*- $\text{Re}(\text{CO})_3(\text{dpkhh})\text{Cl}$ significantly shift to high [22]. For example, in dmsO, the low- and high-energy absorption bands of *fac*- $\text{Re}(\text{CO})_3(\text{dpkhh})\text{Cl}$ were observed at 506 and 398 nm. In the case of dpkhh, the low- and high-energy absorption bands appeared at 400 and 328 nm in dmsO [21]. When a solution of NaBH_4 was added to a solution of *fac*- $\text{Re}(\text{CO})_3(\text{dpkhh})\text{Cl}$ in a polar solvent in the presence and absence of NaBF_4 , the intensity of the low energy band increased and the intensity of the high-energy band decreased (see Fig. 2). The reverse was observed when a solution of NaBF_4 was added to a solution of *fac*- $\text{Re}(\text{CO})_3(\text{dpkhh})\text{Cl}$ or solution of *fac*- $\text{Re}(\text{CO})_3(\text{dpkhh})\text{Cl}$ containing NaBH_4 . This allowed calculations of the extinction coefficients of *fac*- $\text{Re}(\text{CO})_3(\text{dpkhh})\text{Cl}$ in polar solvents and gave ϵ_{440} and ϵ_{318} values of $26\,930 \pm 2000$ and $27\,060 \pm 2000$ $\text{cm}^{-1} \text{M}^{-1}$, respectively, in dmsO. Following a similar procedure, extinction coefficients of $23\,070 \pm 2000$ and $22\,450 \pm 2000$ $\text{cm}^{-1} \text{M}^{-1}$ were calculated at 440 and 318 nm, respectively, in dmf. The electronic absorption spectra of *fac*- $\text{Re}(\text{CO})_3(\text{dpkhh})\text{Cl}$ in polar solvents are temperature dependent, as the temperature increases, the ratio of A_{440}/A_{318} increases, and the reverse was observed when the temperature was allowed to decrease. These results confirmed the reversible interconversion between the high- and low-electronic states of *fac*-

$\text{Re}(\text{CO})_3(\text{dpkhh})\text{Cl}$ and allowed calculations of its thermodynamic activation parameters.¹ A plot of $\ln(A_{440}/A_{318})$ versus $1/T \times 10^3 \text{ K}^{-1}$ gave a straight line with a slope of -494 ± 20 per decade with intercept of $+1.05 \pm 0.05$ that gave changes in enthalpy (ΔH^\ddagger) of $+4.10 \pm 0.20$ kJ mol^{-1} , entropy (ΔS^\ddagger) of $+8.23 \pm 0.45$ kJ mol^{-1} and free energy (ΔG^\ddagger) of $+1.66 \pm 0.20$ kJ mol^{-1} in dmsO. The reversible interconversion between the high and low electronic states of *fac*- $\text{Re}(\text{CO})_3(\text{dpkhh})\text{Cl}$ and its low activation parameters and high value for the extinction coefficient of the electronic states allow for the use of these systems (*fac*- $\text{Re}(\text{CO})_3(\text{dpkhh})\text{Cl}$ and surrounding molecules) as molecular sensors for variety of species in procedures similar to those we reported for the optosensing behavior of dpkhh [21]. The spectra of *fac*- $\text{Re}(\text{CO})_3(\text{dpkhh})\text{Cl}$ in dmsO in the presence and absence of $\text{Mg}(\text{ClO}_4)_2 \cdot n\text{H}_2\text{O}$ are shown in Figs. 3 and 4 shows a plot of the absorbance of *fac*- $\text{Re}(\text{CO})_3(\text{dpkhh})\text{Cl}$ in dmsO in the presence of NaOH and citric acid versus their concentration. When a dmsO solution of NaOH was added to a dmsO solution of the *fac*- $\text{Re}(\text{CO})_3(\text{dpkhh})\text{Cl}$ or a dmsO solution of *fac*- $\text{Re}(\text{CO})_3(\text{dpkhh})\text{Cl}$ containing citric acid, the low-energy absorption band became favorable and when a dmsO solution of citric acid was added to the dmsO solution of *fac*- $\text{Re}(\text{CO})_3(\text{dpkhh})\text{Cl}$ or a dmsO solution of *fac*- $\text{Re}(\text{CO})_3(\text{dpkhh})\text{Cl}$ containing NaOH, the high-energy absorption band became favorable. These results further confirm the reversible interconversion between the low- and high-energy electronic states of *fac*- $\text{Re}(\text{CO})_3(\text{dpkhh})\text{Cl}$ in polar solvents and reveal that chemical species in concentration as low as 1.00×10^{-9} M can be detected and determined using the molecular sensor *fac*- $\text{Re}(\text{CO})_3(\text{dpkhh})\text{Cl}$ in dmsO. A comparison of the optosensing behavior of *fac*- $\text{Re}(\text{CO})_3(\text{dpkhh})\text{Cl}$ with those we reported for dpkhh in non-aqueous media reveal that under the present conditions *fac*- $\text{Re}(\text{CO})_3(\text{dpkhh})\text{Cl}$ is 100 times more sensitive than

¹ For the following interconversion:



Application of Beer's Law gives:

$$A_\alpha/A_\beta = \epsilon_\alpha c_\alpha / \epsilon_\beta c_\beta \quad (2)$$

and

$$\ln(A_\alpha/A_\beta) = \ln(\epsilon_\alpha/\epsilon_\beta) + \ln K \quad (3)$$

The equilibrium constant is related to the thermodynamic parameters as shown in Eq. (4):

$$\ln K = \Delta S^\ddagger / R - \Delta H^\ddagger / RT \quad (4)$$

and substitution of Eq. (4) into Eq. (3) gives:

$$\ln(A_\alpha/A_\beta) = \ln(\epsilon_\alpha/\epsilon_\beta) + \Delta S^\ddagger / R - \Delta H^\ddagger / RT \quad (5)$$

A plot of $\ln(A_\alpha/A_\beta)$ versus $1/T$ gives a straight line with a gradient of $-\Delta H^\ddagger / R$ and an intercept of $\{\ln(\epsilon_\alpha/\epsilon_\beta) + \Delta S^\ddagger / R\}$.

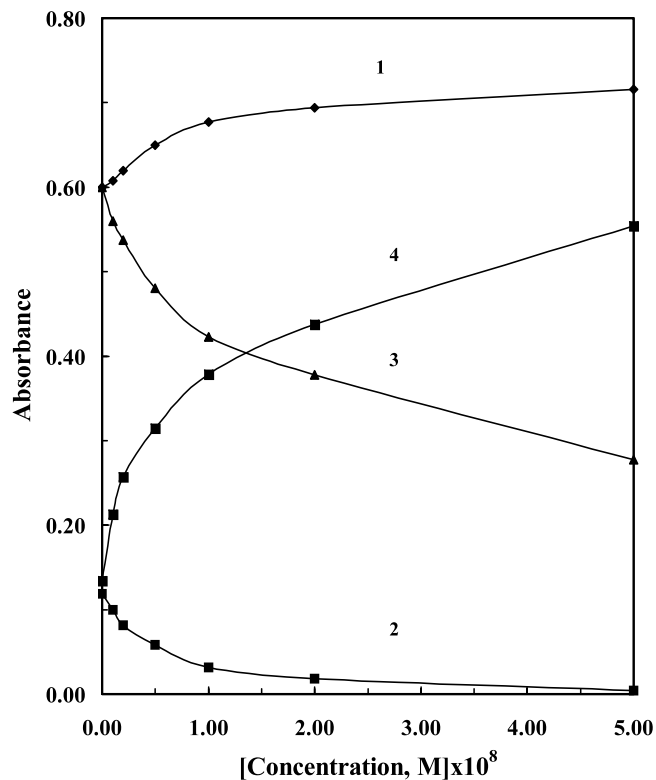


Fig. 4. A plot of A_{440} (1 and 2) and A_{318} of 3.00×10^{-5} M $fac-Re(CO)_3(dpkbh)Cl$ in dmsu versus concentration of NaOH (1,2) and citric acid (3,4).

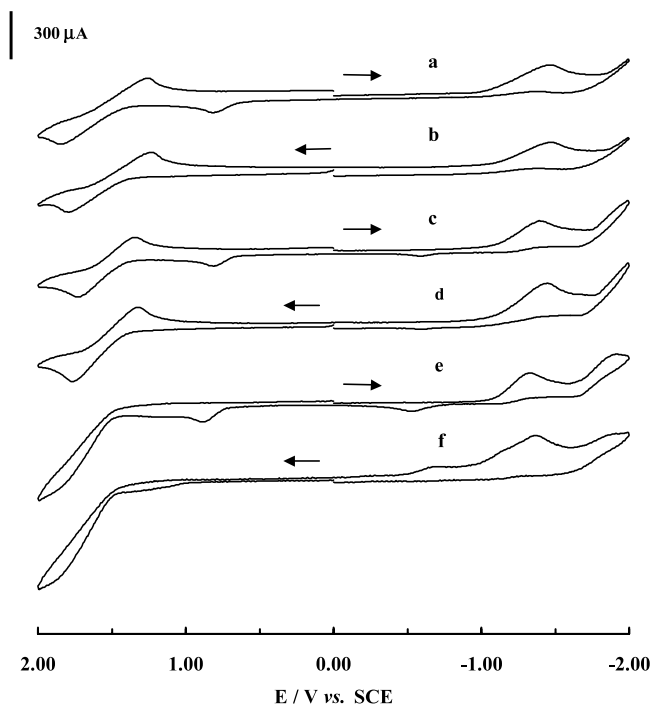


Fig. 5. Cyclic voltammograms of $fac-Re(CO)_3(dpkbh)Cl$ in CH_2Cl_2 (a and b), CH_3CN (c and d) and DMF (e and f) solutions 0.1 M in $[N(n-Bu)_4](PF_6)$ at a glassy carbon working electrode at a scan rate of 400 $mV s^{-1}$ versus SCE.

$dpkbh$ toward metal ions [21]. Further the N,N -coordination of $dpkbh$ in $fac-Re(CO)_3(dpkbh)Cl$ confirm that the optosensing behavior of dpk hydrazones is due to the conformational changes of the hydrazone backbone associated with the solvent–solute interaction.

The electrochemical properties of $fac-Re(CO)_3(dpkbh)Cl$ in non-aqueous media were investigated using voltammetric techniques. Cyclic voltammograms of $fac-Re(CO)_3(dpkbh)Cl$ in CH_2Cl_2 , CH_3CN and dmf are shown in Fig. 5. On reductively initiated scans, irreversible one electron reduction appeared at $E_{p,c} = -1.50$ and -1.43 followed by electrochemically generated product waves at $E_{p,a} = +0.85$, -0.54 and $+0.84$ V and reversible one electron oxidations at $E_{1/2} = +1.55$ and $+1.54$ V in CH_2Cl_2 and CH_3CN , respectively. In dmf , two irreversible reductions appeared at $E_{p,c} = -1.36$ and -1.92 V, reductively generated product waves appeared at $E_{p,a} = -0.5$ and -0.92 V, and an irreversible oxidation appeared at $E_{p,a} = 1.87$ V. On oxidatively initiated scans, the reductively generated product waves disappeared and new oxidatively generated product waves appeared in dmf at $E_{p,c} = -0.64$ and -1.15 V. These voltammograms reveal the sensitivity of $fac-Re(CO)_3(dpkbh)Cl$ to solvent variations and in accord with the electronic absorption spectral properties observed in these solvents. The first reduction wave is assigned to the $Re^{I/0}$ couple and the oxidation wave is assigned to the $Re^{I/II}$ couple, as they fall in the potential observed for these couple in a variety of rhenium carbonyl compounds of polypyridyl-like ligands of the type $fac-Re(CO)_3(L-L)Cl$ where $L-L = dpk$, $dpkoxime$, $dpknph$ and others [12,14,19,22]. For example, in the voltammograms of $fac-Re(CO)_3(dpkphh)Cl$ an irreversible reduction assigned to $Re^{I/0}$ appeared at $E_{p,c} = -1.75$ V in CH_2Cl_2 . The irreversibility of the first electronic reduction and oxidation in dmf and appearance of electrochemically generated product waves hint to rich electrochemical behavior and studies are in progress to explore the electrochemical behavior of $fac-Re(CO)_3(dpkbh)Cl$ in various media in the presence/absence of various substrates and elucidate the mechanism for the redox decomposition of $fac-Re(CO)_3(dpkbh)Cl$ [22].

Single crystals of $fac-Re(CO)_3(dpkbh)Cl$ grown from an acetonitrile solution of $fac-Re(CO)_3(dpkbh)Cl$ are centric in the space group $P\bar{1}$ and single crystals of $fac-Re(CO)_3(dpkbh)Cl \cdot dmsu$ obtained from a $dmsu$ solution of $fac-Re(CO)_3(dpkbh)Cl$ are acentric in the space group $P\bar{1}$. These results confirm the solvent–solute interactions noticed in our solution measurements. Structural analysis revealed the presence of twins of $fac-Re(CO)_3(dpkbh)Cl$ and $fac-Re(CO)_3(dpkbh)Cl \cdot dmsu$. ORTEP drawings of $fac-Re(CO)_3(dpkbh)Cl$ and $fac-Re(CO)_3(dpkbh)Cl \cdot dmsu$ are shown in Fig. 6 and selected bond distances and angles are given in Table 2.

Table 2
Bond lengths (Å) and angles (°) for *fac*-Re(CO)₃(dpkbh)Cl and *fac*-Re(CO)₃(dpkbh)Cl·dmsO

	<i>fac</i> -Re(CO) ₃ (dpkbh)Cl	<i>fac</i> -Re(CO) ₃ (dpkbh)Cl·dmsO
<i>Bond lengths</i>		
Re(1)–C(1)	1.901(11)	1.93(2)
Re(1)–C(2)	1.909(10)	1.926(14)
Re(1)–C(3)	1.900(18)	1.904(9)
Re(1)–N(1)	2.209(7)	2.20(2)
Re(1)–N(2)	2.189(7)	2.154(19)
Re(1)–Cl(1)	2.457(4)	2.485(7)
Re(1')–C(1')	1.938(15)	1.93(3)
Re(1')–C(2')	1.930(18)	1.910(9)
Re(1')–C(3')	1.946(9)	1.910(9)
Re(1')–N(1')	2.221(10)	2.210(15)
Re(1')–N(2')	2.149(11)	2.242(18)
Re(1')–Cl(1')	2.455(2)	2.459(7)
N(3)–C(4)	1.258(16)	1.21(3)
N(3)–N(4)	1.374(11)	1.41(2)
N(4)–C(5)	1.37(2)	1.47(3)
C(5)–O(4)	1.230(15)	1.14(3)
N(3')–C(4')	1.283(11)	1.33(2)
N(3')–N(4')	1.368(10)	1.29(3)
N(4')–C(5')	1.347(15)	1.38(4)
C(5')–O(4')	1.236(14)	1.29(3)
S(1)–O(6)		1.49(3)
S(1')–O(6')		1.36(2)
<i>Bond angles</i>		
C(3)–Re(1)–C(1)	90.2(6)	91.9(10)
C(1)–Re(1)–C(2)	87.8(4)	91.9(9)
C(3)–Re(1)–N(2)	91.6(4)	92.1(9)
C(1)–Re(1)–N(2)	95.9(4)	92.8(8)
C(2)–Re(1)–N(2)	176.2(3)	173.8(8)
C(3)–Re(1)–N(1)	93.1(4)	94.4(10)
N(2)–Re(1)–N(1)	83.4(3)	81.7(8)
C(3)–Re(1)–Cl(1)	175.5(3)	177.1(9)
N(1)–Re(1)–Cl(1)	84.3(3)	83.2(6)
C(2')–Re(1')–C(1')	87.8(7)	85.8(10)
C(1')–Re(1')–C(3')	90.1(5)	87.2(11)
C(2')–Re(1')–N(2')	176.1(4)	173.7(7)
C(1')–Re(1')–N(2')	95.6(6)	92.4(10)
C(3')–Re(1')–N(2')	92.5(4)	93.8(10)
C(2')–Re(1')–N(1')	93.0(5)	97.7(7)
C(1')–Re(1')–N(1')	176.6(3)	176.5(11)
C(3')–Re(1')–N(1')	93.1(4)	93.2(9)
N(2')–Re(1')–N(1')	83.5(4)	84.0(6)
C(3')–Re(1')–Cl(1')	175.8(4)	175.9(10)
N(1')–Re(1')–Cl(1')	84.32(19)	85.8(4)
C(4)–N(3)–N(4)	121.4(10)	116.1(19)
N(3)–N(4)–C(5)	121.0(10)	110.2(15)
O(4)–C(5)–N(4)	118.2(13)	127.6(19)
N(4')–N(3')–C(4')	120.7(7)	117.2(16)
N(3')–N(4')–C(5')	120.4(8)	123.1(18)
O(4')–C(5')–N(4')	120.0(11)	115(2)

The bond distances and angles are normal and similar to those we reported for *fac*-Re(CO)₃(dpknph)Cl·dmsO, *fac*-Re(CO)₃(dpkphh)Cl·CH₃CN, dpkbh and other related compounds [16–19,21–24]. The coordination about rhenium is distorted octahedral with the *N,N*-bidentate dpkbh forming a six membered (Re_x–N1_x–C15_x–C00_x–C25_x–N2_x where *x* = 1,1', 2 or 2') me-

talocyclic ring with the pyriding rings in a butterfly (Λ) formation. The N–N bite angles [\angle N(1)_{*x*}–Re_{*x*}–N(2)_{*x*}] (see Table 2) are of the same order as the 81.6° and 84.6° bite angles observed for the same bite angles in *fac*-Re(CO)₃(dpkO,OH) [18] and ReOCl₂(dpkO,OH) [32], respectively, and is larger than those reported for a variety of rhenium compounds of α -diimine ligands of

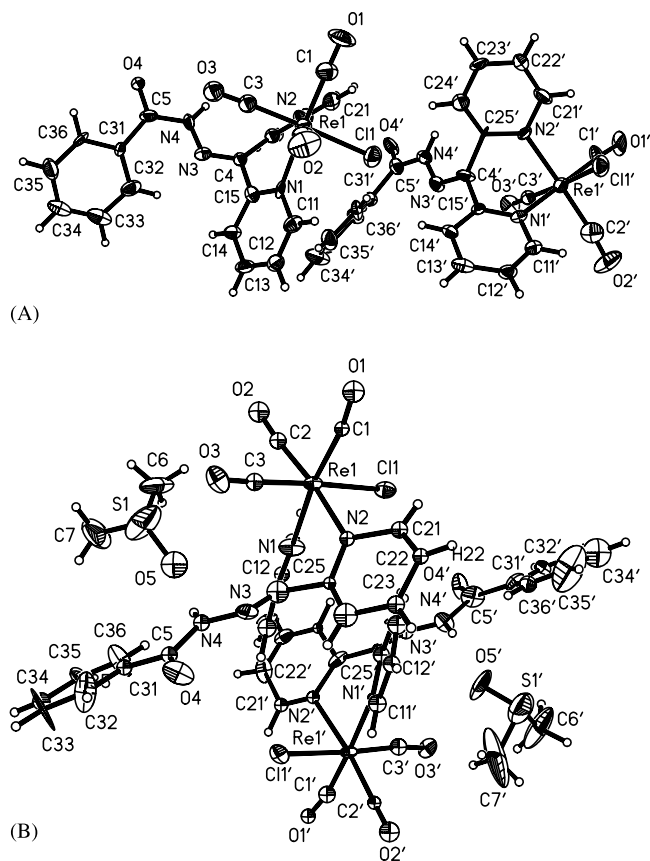


Fig. 6. ORTEP drawings of (a) *fac*- $\text{Re}(\text{CO})_3(\text{dpkbbh})\text{Cl}$ and (b) *fac*- $\text{Re}(\text{CO})_3(\text{dpkbbh})\text{Cl}\cdot\text{dmsO}$. The thermal ellipsoids are drawn at the 30% probability level.

the type *fac*- $\text{Re}(\text{CO})_3(\text{L-L})\text{Cl}$ [33–38], for example, in *fac*- $\text{Re}(\text{CO})_3(\text{bipy})(\text{OPOF}_2)$ has a $\angle \text{N}(1)-\text{Re}1-\text{N}(1\text{A}) = 74.3^\circ$ [37]. These results confirm that the six membered metallocyclic ring in rhenium compounds of polypyridyl-like ligands is more stable than the five-membered metallocyclic ring in rhenium compounds of α -diimine ligands. The amide NH and CO groups of the hydrazone moiety in *fac*- $\text{Re}(\text{CO})_3(\text{dpkbbh})\text{Cl}$ are in anti-position and the hydrazone moiety is non-planar while in *fac*- $\text{Re}(\text{CO})_3(\text{dpkbbh})\text{Cl}\cdot\text{dmsO}$ the amide NH and CO groups of are in syn position and the hydrazone moiety is semi-planar (see Fig. 6). These results confirm the proposed conformational changes due to solvent–solute interactions noticed in our solution measurements and reveal that the low energy electronic state is due to the syn conformation associated with the solvent–solute interaction and the high-energy electronic state is due to the anti-conformation due to solvent free interaction. This is consistent with our optical measurements as in non-polar solvent such as CH_2Cl_2 a high-energy electronic state appeared at ~ 310 nm and in polar coordinating solvent two electronic states appeared at ~ 440 and ~ 318 nm (Fig. 6).

The packing of molecules (Fig. 7) reveals stacks of non-helical *fac*- $\text{Re}(\text{CO})_3(\text{dpkbbh})\text{Cl}$ and helical *fac*-

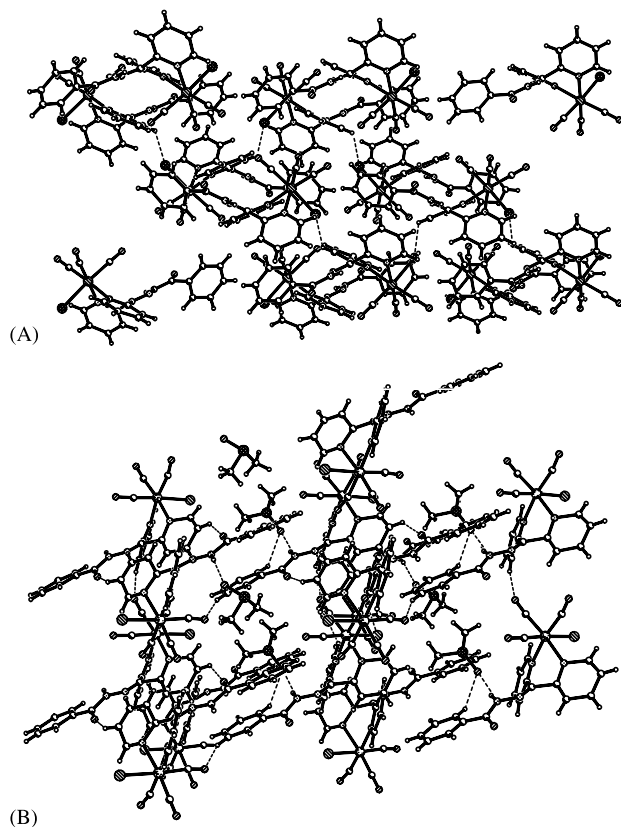


Fig. 7. Packing diagrams of (a) *fac*- $\text{Re}(\text{CO})_3(\text{dpkbbh})\text{Cl}$ and (b) *fac*- $\text{Re}(\text{CO})_3(\text{dpkbbh})\text{Cl}\cdot\text{dmsO}$. Non-covalent bonds are denoted by dashed line.

Table 3

Bond lengths (Å) and angles ($^\circ$) for *fac*- $\text{Re}(\text{CO})_3(\text{dpkbbh})\text{Cl}$ and *fac*- $\text{Re}(\text{CO})_3(\text{dpkbbh})\text{Cl}\cdot\text{dmsO}$

D–H...A	d(D–H)	d(H...A)	d(D...A)	$\angle(\text{DHA})$
<i>fac</i> - $\text{Re}(\text{CO})_3(\text{dpkbbh})\text{Cl}$				
$\text{N}(4)-\text{H}(4)\cdots\text{O}(4)^1$	0.86	2.08	2.85(1)	147.23
$\text{N}(4)-\text{H}(4)\cdots\text{O}(4)^2$	0.86	2.11	2.87(1)	145.38
$\text{C}(14')-\text{H}(14')\cdots\text{Cl}(1)$	0.93	2.83	3.53(1)	133.50
$\text{C}(22')-\text{H}(22')\cdots\text{O}(3)^3$	0.93	2.60	3.27(1)	129.58
$\text{C}(32)-\text{H}(32)\cdots\text{N}(3)$	0.93	2.45	2.86(2)	106.96
$\text{C}32'-\text{H}(32')\cdots\text{N}(3')$	0.93	2.47	2.88(1)	106.73
<i>fac</i> - $\text{Re}(\text{CO})_3(\text{dpkbbh})\text{Cl}\cdot\text{dmsO}$				
$\text{N}(4)-\text{H}(4)\cdots\text{O}(5)$	0.86	1.98	2.78(3)	154.81
$\text{N}(4)-\text{H}(4)\cdots\text{O}(5')$	0.86	2.20	3.00(3)	155.82
$\text{C}(11')-\text{H}(11')\cdots\text{Cl}(1)^4$	0.93	2.82	3.66(3)	150.26
$\text{C}(14)-\text{H}(14)\cdots\text{O}(2)^4$	0.93	2.43	3.31(3)	159.48
$\text{C}(22)-\text{H}(22)\cdots\text{O}(4)^5$	0.93	2.50	3.17(3)	129.46
$\text{C}(22')-\text{H}(22')\cdots\text{O}(4)^6$	0.93	2.39	3.11(3)	134.51
$\text{C}(33)-\text{H}(33)\cdots\text{O}(3)^7$	0.93	2.57	3.41(3)	151.51
$\text{C}(36)-\text{H}(36)\cdots\text{O}(5)$	0.93	2.42	3.16(3)	135.70

Symmetry transformations used to generate equivalent atoms: 1 = $1-x, 1-y, -z$, 2 = $1-x, 2-y, -z$, 3 = $-x, 1-y, -z$, 4 = $1+x, y, z$, 5 = $x, y, 1+z$, 6 = $x, y, -1+z$ and 7 = $x, -1+y, 1+z$.

$\text{Re}(\text{CO})_3(\text{dpkbbh})\text{Cl}\cdot\text{dmsO}$ units interlocked via a web of hydrogen bonds (see Table 3 and Figs. 7 and 8). The crystallized dmsO molecules are not equivalent, in

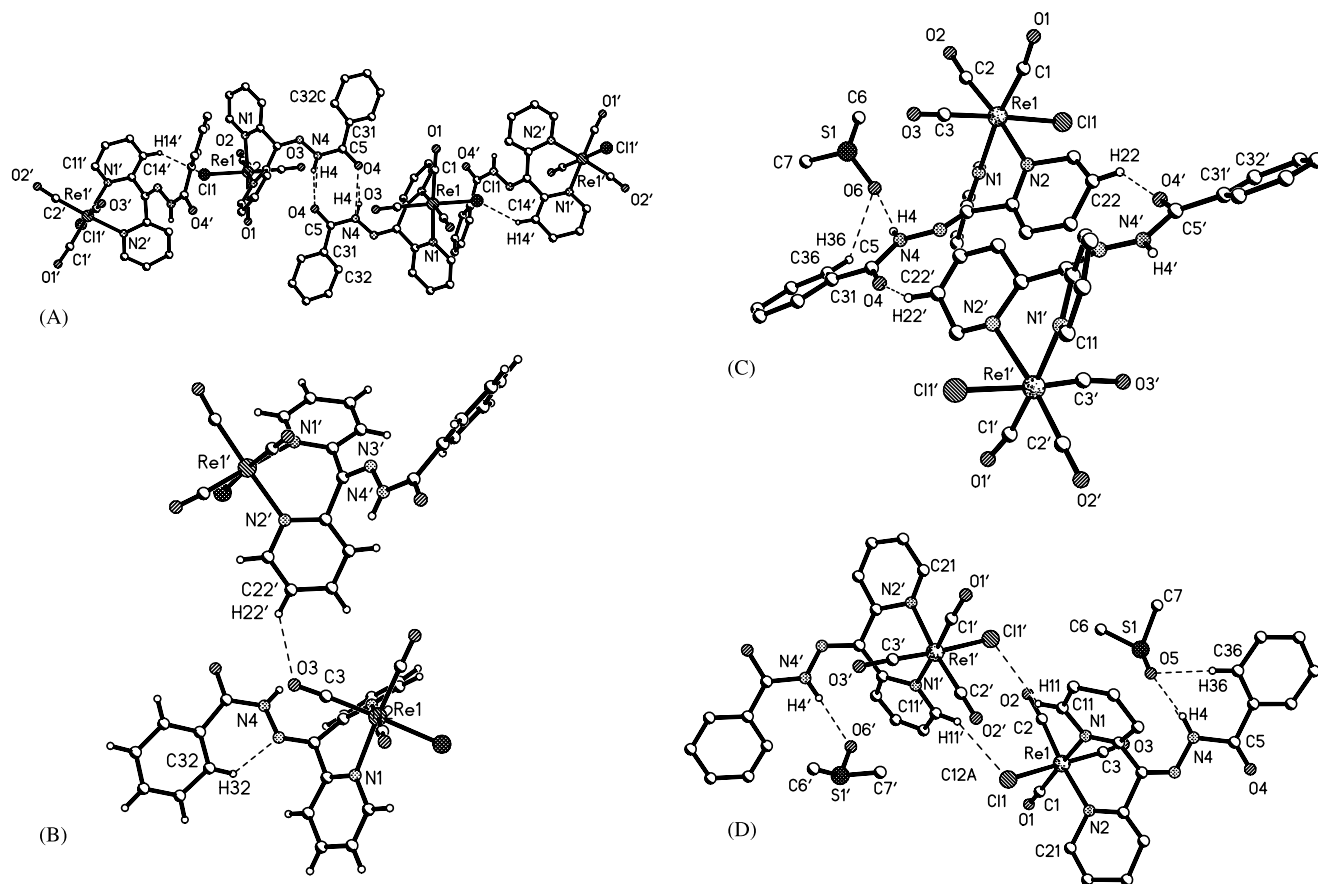


Fig. 8. Views of the hydrogen bonding in *fac*- $\text{Re}(\text{CO})_3(\text{dpkbh})\text{Cl}$ (a and b) and *fac*- $\text{Re}(\text{CO})_3(\text{dpkbh})\text{Cl}\cdot\text{dmsO}$ (c and d). Non-covalent bonds are denoted by dashed line.

residue *fac*- $\text{Re}(\text{CO})_3(\text{dpkbh})\text{Cl}\cdot\text{dmsO}$ a three centered bifurcated hydrogen bond is formed between dmsO oxygen atom and amide N4 and aromatic C36 protons (see Table 3 and Fig. 8(c)) and in residue [*fac*- $\text{Re}(\text{CO})_3(\text{dpkbh})\text{Cl}\cdot\text{dmsO}$] two centered linear hydrogen bond is formed between O5 and the amide (N4–H4) proton of the hydrazone moiety (see Table 3 and Fig. 8(d)). The hydrogen bond between the hydrazone N3 of *fac*- $\text{Re}(\text{CO})_3(\text{dpkbh})\text{Cl}$ and aromatic C32 proton appears to reinforce the syn conformation of the hydrazone amide moiety and the hydrogen bond between the carbonyl group and the aromatic C22 proton of the pyridyl ring appears to reinforce the anti-conformation of the amide moiety of the hydrazone backbone. The bond distances and angles of the hydrogen bonds are normal and similar to those reported for a variety of compounds containing such interactions [16–19,21–24,39–42].

Owing their convenient synthesis, rich physico-chemical properties, potential use in non-linear optics and molecular sensing work is in progress to isolate a variety of metal compounds of polypyridyl-like ligands to explore their electro-optical properties, solid state structures and conformations.

4. Conclusion

The isolation of *fac*- $\text{Re}(\text{CO})_3(\text{dpkbh})\text{Cl}$ marks the first instance a metal compound of *N,N*-bidentate dpkbh has been reported. Spectroscopic and electrochemical measurements on *fac*- $\text{Re}(\text{CO})_3(\text{dpkbh})\text{Cl}$ revealed strong solvent–solute interaction and structural studies on *fac*- $\text{Re}(\text{CO})_3(\text{dpkbh})\text{Cl}$ and *fac*- $\text{Re}(\text{CO})_3(\text{dpkbh})\text{Cl}\cdot\text{dmsO}$ reveal octahedral coordination about rhenium and different conformations about the amide of the hydrazone moiety. The packing of molecules reveals a web of hydrogen bonds that may account for the different conformational forms in the solid state.

Acknowledgements

I acknowledge funding from The University of the West Indies (UWI) and Inter-America Development Bank (IDB) for funds to establish the X-ray Laboratory at UWI-Mona.

References

- [1] Z.E. Serna, R. Cortés, M.K. Urtiaga, M.G. Barandika, L. Lezama, M.I. Arriortua, T. Rojo, *Eur. J. Inorg. Chem.* (2001) 865.
- [2] G. Yang, S.-L. Zheng, X.-M. Chen, H.K. Lee, Z.-Y. Zhou, T.C.W. Mak, *Inorg. Chim. Acta* 303 (2000) 86.
- [3] H. Bock, T.T.H. Van, H. Schödel, R. Dienelt, *Eur. J. Org. Chem.* (1998) 585.
- [4] S.R. Breeze, S. Wang, J.E. Greedan, N.P. Raju, *Inorg. Chem.* 35 (1996) 6944.
- [5] H.-L. Kwong, L.-S. Cheng, W.-S. Lee, W.-L. Wong, W.-T. Wong, *Eur. J. Inorg. Chem.* (2000) 1997.
- [6] M.A.S. Goher, F.A. Mautner, *Polyhedron* 18 (1999) 3425.
- [7] S.O. Sommerer, C.E. MacBeth, A.J. Jircitano, K.A. Abboud, *Acta Crystallogr. Sect. C* 53 (1997) 1551.
- [8] S.O. Sommerer, B.L. Westcott, A.J. Jircitano, K.A. Abboud, *Inorg. Chim. Acta* 238 (1995) 149.
- [9] L.H.S.A. Terra, M.C. Da Cunha Areias, I. Gaubeur, M.E.V. Suarez-Iha, *Spectrosc. Lett.* 32 (1999) 257.
- [10] M. Carcelli, C. Pelizzi, G. Pelizzi, P. Mazza, F. Zani, Franca, J. *Organomet. Chem.* 488 (1995) 55.
- [11] M. Bakir, J.A.M. McKenzie, *J. Chem. Soc., Dalton Trans.* (1997) 3571.
- [12] M. Bakir, J.A.M. McKenzie, *Electroanal. Chem.* 425 (1997) 61.
- [13] M. Bakir, *J. Electroanal. Chem.* 466 (1999) 60.
- [14] M. Bakir, K. Abdur-Rashid, *Trans. Metal Chem.* 24 (1999) 384.
- [15] M. Bakir, K. Abdur-Rashid, W.H. Mulder, *Talanta* 51 (2000) 735.
- [16] M. Bakir, *Acta Crystallogr. Sect. C* 57 (2001) 1154.
- [17] M. Bakir, *Acta Crystallogr. Sect. C* 57 (2001) 1371.
- [18] M. Bakir, *Acta Crystallogr. Sect. C* 58 (2002) m74.
- [19] M. Bakir, *Eur. J. Inorg. Chem.* (2002) 481.
- [20] M. Bakir, C. Gyles, *Talanta* 56 (2002) 1117.
- [21] M. Bakir, O. Brown, *J. Mol. Struct.* 609 (2002) 129.
- [22] M. Bakir, *Inorg. Chim. Acta* 332 (2002) 1.
- [23] M. Bakir, O. Green, *Acta Crystallogr. Sect. C* 58 (2002) 0263.
- [24] M. Bakir, O. Brown, *J. Mol. Struct.* 641 (2002) 183.
- [25] J. Ellena, G. Punte, B.E. Rivero, *J. Chem. Crystallogr.* 26 (1996) 319.
- [26] M.C. Etter, *Acc. Chem. Res.* 23 (1990) 120.
- [27] F. Pan, C. Bosshard, M.S. Wong, C. Serbutoviez, K. Schenk, V. Gramlich, P. Gunter, *Chem. Mater.* 9 (1997) 1328.
- [28] C. Bosshard, K. Sutter, P. Pretre, J. Hullinger, M. Florsheimer, P. Kaatz, P. Gunter, *Organic Nonlinear Optical Materials*, Gordon and Breach Science Publishers, Amsterdam, 1995.
- [29] Bruker-SHELXTL, Software version 5.1, Bruker AXS, Madison, Wisconsin, USA, 1997.
- [30] G.M. Sheldrick, SHELX97 and SHELXL97, University of Göttingen, Germany, 1997.
- [31] F.L. Boschke, W. Fresenius, J.F.K. Huber, E. Pungor, G.A. Rechnitz, W. Simon, Th.S. West (Eds.), *Tables of Spectral data for Structure Determination of Organic*, Springer, Berlin, Heidelberg, 1983.
- [32] T.I.A. Gerber, H.J. Kemp, J.G.H. du Preez, G. Bandoli, *J. Coord. Chem.* 28 (1993) 329.
- [33] V.W.-W. Yam, K.K.-W. Lo, K.-K. Cheung, R.Y.-C. Kong, *J. Chem. Soc., Chem. Commun.* (1995) 1191.
- [34] D.H. Gibson, B.A. Sleadd, X. Yin, A. Vij, *Organometallics* 17 (1998) 2689.
- [35] V.W.-W. Yam, K.-Z. Wang, C.-R. Wang, Y. Yang, K.-K. Cheung, *Organometallics* 17 (1998) 2440.
- [36] V.W.-W. Yam, V.C.-Y. Lau, K.-K. Cheung, *Organometallics* 14 (1995) 2749.
- [37] E. Horn, M.R. Snow, *Aust. J. Chem.* 33 (1980) 2369.
- [38] J.C. Calabrese, W. Tam, *Chem. Phys. Lett.* 133 (1987) 244.
- [39] D. Braga, F. Grepioni, G.R. Desiraju, *Chem. Rev.* 98 (1998) 1375.
- [40] J.P. Glusker, M. Lewis, M. Rossi, *Crystal Structure Analysis for Chemists and Biologists*, Wiley-VCH, New York, 1994.
- [41] J.H. Williams, *Acc. Chem. Res.* 26 (1993) 593.
- [42] G.R. Desiraju, *Crystal Engineering*, Elsevier, New York, 1989.